Targeting 14-3-3ζ overcomes resistance to EGFR-TKI in lung adenocarcinoma via BMP2/Smad/ID-1 signaling

Jinfang Cui
Tumor Hospital of Harbin Medical University
Yang Song
Second Affiliated Hospital of Harbin Medical University
Xuejiao Han
Tumor Hospital of Harbin Medical University
Jing Hu
Tumor Hospital of Harbin Medical University
Yanbo Chen
Tumor Hospital of Harbin Medical University
Xuesong Chen
Tumor Hospital of Harbin Medical University
Xiaomin Xu
Tumor Hospital of Harbin Medical University
Ying Xing
Tumor Hospital of Harbin Medical University
Hailing Lu (luhailing2004@163.com)
Tumor Hospital of Harbin Medical University https://orcid.org/0000-0001-5304-5358
Li Cai
Tumor Hospital of Harbin Medical University

Research

Keywords: 14 3 3ζ, lung adenocarcinoma, EGFR TKI resistance, BMP2/Smad/ID 1 signaling, signaling pathway

Posted Date: February 17th, 2020

DOI: https://doi.org/10.21203/rs.2.23664/v1

Original Article

Targeting 14-3-3ζ overcomes resistance to EGFR-TKI in lung adenocarcinoma via BMP2/Smad/ID-1 signaling

Running title: 14-3-3ζ knockdown attenuates EGFR-TKI resistance

Jinfang Cui[1†], Yang Song[2†], Xuejiao Han[1†], Jing Hu[1], Yanbo Chen[1], Xuesong Chen[1], Xiaomin Xu[1], Ying Xing[1], Hailing Lu[1*], Li Cai[1*]

1 The Fourth Department of Medical Oncology, Harbin Medical University Cancer Hospital, 150 Haping Road, Harbin, 150040, China;

2 Department of Orthopedic Surgery, The Second Affiliated Hospital of Harbin Medical University, Xuefu Road 246, Harbin, 150081, China.

[†]Jinfang Cui, Yang Song and Xuejiao Han contributed equally to this work.

[*]**Corresponding author: Hailing Lu and Li Cai**

Hailing Lu, The Fourth Department of Medical Oncology, Harbin Medical University Cancer Hospital, 150 Haping Road, Harbin, 150040, China. Tel.: +86 451 86298038; Fax: +86 451 86298735; E-mail: luhailing2004@163.com.

Li Cai, The Fourth Department of Medical Oncology, Harbin Medical University Cancer Hospital, 150 Haping Road, Harbin, 150040, China. Tel.: +86 451 86298038; Fax: +86 451 86298735; E-mail: caili@ems.hrbmu.edu.cn.

co-authors' Email:

Jinfang Cui, cuijinfang0502@163.com;

Yang Song, sy13945697231@163.com;

Xuejiao Han, xuejiao_han@126.com.

Keywords

14-3-3ζ; lung adenocarcinoma; EGFR-TKI resistance; BMP2/Smad/ID-1 signaling signaling pathway

Abstract

Background: 14-3-3ζ protein which acts as a putative oncoprotein has been found to promote proliferation, metastasis and chemoresistance of cancer cells in several cancers including lung adenocarcinoma (LUAD), however, its significance in epidermal growth factor receptor-tyrosine kinase inhibitor (EGFR-TKI) resistance

remains unknown.

Methods: The Cancer Genome Atlas (TCGA) database was used to determine 14-3-3ζ expression in pan-cancer and LUAD. 14-3-3ζ and ID1 expression was then examined in clinical LUAD samples by immunohistochemistry (IHC). Lentiviral transfection with 14-3-3ζ-specific shRNA was used to establish stable 14-3-3ζ knockdown gefitinib resistant PC9 (PC9/GR) and H1975 cell lines. The effect of 14-3-3ζ knockdown on reversing EGFR-TKI resistance was determined in vitro by CCK-8, wound healing, transwell assays and flow cytometry. A xenograft tumor model was established to evaluate the role of 14-3-3ζ in EGFR-TKI resistance. Microarray analysis results showed the multiple pathways regulated by 14-3-3ζ-shRNA.

Results: In the present study, we firstly demonstrated that 14-3-3ζ expression was elevated and predicted unfavourable prognosis in pan-cancer including LUAD based on TCGA. In addition, high 14-3-3ζ expression was significantly associated with advanced T stage, TNM stage, present of lymph node metastasis and, importantly, poor treatment response to EGFR-TKI in LUAD patients with EGFR-activating mutations. 14-3-3ζ shRNA significantly sensitized EGFR-TKI-resistant human LUAD cells to gefitinib and, notably, reversed epithelial-to-mesenchymal transition (EMT). BMP signaling activation was decreased in EGFR-TKI resistant cells followed by 14-3-3ζ depletion in microarray analysis, which was further validated by Western blot analysis. Furthermore, the expression of 14-3-3ζ positively correlates with ID1 expression in human EGFR-mutant LUAD patient samples. *In vivo*, 14-3-3ζ shRNA and gefitinib treatment resulted in a significant reduction in the tumor burden compared to that treated with gefitinib alone.

Conclusion: Our work uncovers a hitherto unappreciated role of 14-3-3ζ in EGFR-TKI resistance. This study might provide a potential therapeutic approach for treating LUAD patients harboring EGFR mutations.

Background

Lung cancer remains the leading causes of cancer death worldwide and most of the lung cancer is non-small cell lung cancer (NSCLC) pathologically [1, 2]. NSCLC also

is a heterogeneous disease typically classified into three broad subtypes, lung adenocarcinoma (LUAD), squamous cell carcinoma (LUSC) and large cell carcinoma [3, 4]. LUAD is a devastating disease because of the dismal patient survival [5]. Encouragingly, epidermal growth factor receptor-tyrosine kinase inhibitor (EGFR-TKI), such as gefitinib and erlotinib, leads to unprecedented clinical benefits and provide a new weapon against LUAD with EGFR-activating mutations [6]. However, most of LUAD patients eventually develop acquired resistance to EGFR-TKI [6]. Hence the exploring of the molecular mechanism involved in EGFR-TKI resistance and developing innovative treatment strategies are urgently needed.

The human 14-3-3 proteins share highly conserved homology and are comprised of 7 isoforms (β, σ, ε, τ/θ, γ, η and ζ) with unique expression patterns in different cell types and tissues [7]. Of the seven isoforms in eukaryotic organisms, 14-3-3ζ (also known as YWHAZ) has been proposed to be directly involved in cellular transformation and proliferation [8]. Importantly, accumulating evidences have disclosed that 14-3-3ζ played key roles in the regulation of diverse diseases, such as obesity [9], diabetes [10] and cancer [11]. 14-3-3ζ functions as a central node to regulate the critical processes in cancer including cell motility, metabolism, cycle progression, mitogenic, apoptosis and epithelial-to-mesenchymal transition (EMT) by oncogenic signalling pathways [8, 11-17]. However, to our knowledge, the role of 14-3-3ζ in EGFR-TKI resistance remains unknown.

Bone morphogenetic proteins (BMPs) were one of the transforming growth factor-beta (TGF-β) subfamilies and they used similar signal transduction pathways that involve transmembrane serine threonine kinase receptors and Smad proteins [18]. Among of BMPs, overexpreesion of BMP-2 was proven to occur in approximately 98% of lung carcinomas and contribute to lung cancer progression [19-21]. BMP2 could trigger the phosphorylation of Smad1/5 via binding to the receptors, and activated Smad1/5 binds Smad4, translocates to the nucleus, binds to Smad-binding elements in the the inhibitors of differentiation 1 (ID1) promoter, and induces ID1 transcription [22]. ID1 promotes tumorigenesis, EMT and metastasis of various

cancer types including lung cancer [23-26]. The mechanism of regulation of BMP2/Smad/ID1 signaling pathway still needs to be further explicated.

In the present study, we provided evidence that 14-3-3ζ inhibition significantly attenuated LUAD cells refractory to EGFR-TKI *in vitro* and *in vivo*, which was accompanied by EMT reversal. We performed global gene expression microarray profiling in EGFR-TKIs-resistant cells after shRNA knockdown of 14-3-3ζ and analyzed the gene expression data. Here, we demonstrted that 14-3-3ζ has a positively regulatory effect on the BMP2/Smad/ID1 signaling pathway. Our findings suggest that 14-3-3ζ might be a novel and potential target for overcoming EGFR-TKIs resistance in LUAD with an EGFR-activating mutation.

Materials and methods

Bioinformatics analysis

We used web-based tools available through GEPIA (Gene Expression Profiling Interactive Analysis, http://gepia.cancerpku.cn/) based on the TCGA and GTEx database to detect 14-3-3ζ mRNA levels in various tumors. The KaplanMeier Plotter (http://kmplot.com/analysis/) online tool was used to test the predictive significance of 14-3-3ζ expression.

Cell lines and tissue specimens

The human NSCLC cell lines PC-9, PC-9/GR and NCI-H1975 were obtained from Heilongjiang Cancer Institute (Harbin, China) (PC-9/GR: stable gefitinib-resistant PC-9 cells). The cells were cultured in RPMI-1640 and DMEM. Both media were supplemented with 10% heat-inactivated fetal bovine serum (Hyclone), 100 units/mL penicillin and 100μg/mL streptomycin (Gibco). The cells were grown in an incubator at 37°C with 5% CO_2. Cell lines were periodically authenticated by STR profiling, and detected as no mycoplasma contamination using previously reported methods.

The tissue used in the study was derived from patients whose pathological tissue type was diagnosed as LUAD at the Affiliated Tumor Hospital of Harbin Medical University. Between November 2009 and December 2017, 159 patients with EGFR mutant LUAD were enroled into this retrospective study, including 41 patients treated with EGFR-TKIs. Formalin-fixed, paraffin-embedded tissue and complete clinical

records of patients were collected. In addition, ten paired samples of primary LUAD and matched adjacent tissues were stored frozen, which were obtained from patients undergoing lung cancer surgery at the Affiliated Tumor Hospital of Harbin Medical University. The study protocol was explained to the patients in detail and each patient signed a written informed consent forms for medical record review and tissue sample donation. Ethical clearance and approval was obtained from the Ethics Review Committee at Harbin Medical University.

Immunohistochemistry (IHC)

IHC analysis was performed to detect the expression of 14-3-3ζ and ID1 in paraffin sections. Immunohistochemical SP method for staining, the main steps were as follows: slices were baked in a 70°C oven for 3 h; dewaxed with xylene, hydrated with gradient alcohol (100%, 95%, 90%, 85%, 80%); Inactivated by immersion in 3% H_2O_2 for 10 min. The sections were subsequently submerged in EDTA (pH 8) and autoclave at 121°C for 5 min to retrieve the antigenicity and cooled at room temperature. After washing with PBS, the sections were incubated with primary antibody 14-3-3ζ (Santa Cruz Biotechnology, SC-293415, diluted at 1:100), ID1 (Santa Cruz Biotechnology, SC-374287, diluted at 1: 100) overnight at 4 °C. Then the sections were incubated with anti-horseradish peroxidase- labeled goat anti-rabbit IgG antibody at room temperature for 30 min; DAB coloration, tap water rinse; hematoxylin counterstaining, dehydration, transparency, and mounting. Under light microscopy, the cells showed yellow or brownish yellow fine particles as a positive reaction. According to the cell staining intensity: no coloring is 0 points, light yellow is 1 point, yellow is 2 points, brown is 3 points. According to the percentage of positive cells: ≤ 5% is 0, 6% to 25% is 1 point, 26% to 50% is 2 points, 51% to 75% is 3 points, ≥ 76% is 4 points. Add the two scores, 0 (-), 1 to 2 (+), 3 to 4 (++), and 5 to 7 (+++). Set (-) ~ (+) to low expression and (++) to (+++) to high expression. The above results were confirmed by at least two pathologists in a double-blind case.

Western blot analysis

Total proteins from the human LUAD cells or frozen lung tissues were extracted using RIPA lysis buffer (Beyotime) containing a 1% protease inhibitors (Roche).

Protein concentration was measured with a bicinchoninic acid kit (Clontech), and protein samples were separated by 12% SDS–polyacrylamide gel electrophoresis and transferred to a PVDF membrane (Whatman, Maidstone, Kent, UK). The PVDF membranes containing target protein were blocked with skim milk. Blots were then probed with primary antibodies overnight at 4°C. Membranes were washed with PBS containing 0.05% Tween-20 (PBS-T) and then incubated with horseradish peroxidase-conjugated anti-mouse and-rabbit secondary antibodies (Amersham Pharmacia Biotech, Piscataway, NJ; diluted 1:5000). Protein bands were visualized using an enhanced chemiluminescence (ECL) system (Amersham Pharmacia Biotech) according to the manufacturer's instructions. The primary antibodies used for the western blot analyses were as follows: 14-3-3ζ (Santa Cruz Biotechnology, SC-293415, diluted at 1: 500), E-cadherin (Abcam, ab133597, diluted at 1: 5000), N-cadherin (Abcam, ab76057, diluted at 1: 1000), Vimentin (Abcam, ab137321, diluted at 1: 1500), BMPR2 (Abcam, ab124463, diluted at 1: 500), Smad1 (Cell Signaling Technology, #6944, diluted at 1: 1000), Smad5 (Cell Signaling Technology, #9517, diluted at 1: 1000), phosphorylated (p)-Smad1/5 (Cell Signaling Technology, #9516, diluted at 1: 1000), ID1 (Santa Cruz Biotechnology, SC-374287, diluted at 1: 500) and β-actin (used as the loading control; Sigma, A1978). Western blot bands were quantified by the Image J software (U.S. National Institutes of Health, USA). The experiment was repeated thrice.

Wound-healing assay

Cells with a density of 1×10^6 cells/well were seeded in six-well plates. When cells were grown to 80% to 90% confluence a cross-shaped wound was scratched by dragging a 10μl sterile pipette tip across the monolayers of cells, and the cell debris was rinsed with PBS. The process of wound healing was then observed at time 0, 24, and 48 hour, and the cells were stained with crystal violet at 48 hours for a clearer view of the wound. Three replicate wells were used for each condition, and three cell images of per well were captured by an inverted fluorescence microscope for quantifcation analysis.

Cell migration and invasion assay

Cell migration and invasion assay were performed using 24-well transwell plates (Corning Inc., Corning, NY). Matrigel (BD Biosciences, USA) was placed on an ice plate and matched with 1640 or DMEM at a ratio of 1:7. 30ul of treated matrigel was pipetted on the bottom of upper chamber, taking care to prevent air bubbles, and then placing the transwell in a 37°C incubator containing 5% CO_2 for 1 to 2 hour. During this time, a cell suspension was prepared using serum-free medium, and seeded into the upper chamber at a density of 4×10^3 cells/200 ul per well, and 600 ul of medium containing 10% fetal bovine serum was added to the lower chambers. Cells were incubated for 24 hours and 48 hours, respectively, in a transwell without pre-applied matrigel and pre-coated matrigel. The cells in the upper chambers were wiped clean with a cotton swab, and the cells that had migrated to the lower surface of the membrane were fixed with methanol for 1 hour, stained with crystal violet for 30 minutes. The cells were photographed under an inverted fluorescence microscope after staining solution was washed off with PBS. The number of invaded cells per field view was counted using the cell counter plugins in Image J. All experiments were performed in triplicate.

Retroviral infection and transfection

Lentiviruses containing shRNA targeting 14-3-3ζ were purchased from Shanghai GeneChem (Genechem Co., Ltd, Shanghai, China). The sh14-3-3ζ target sequence was 5′-TCGAGAATACAGAGAGAAA -3′. H1975 and PC9/GR cells were infected with lentiviral particles and cultured in complete 1640 or DMEM containing puromycin (Santa Cruz Biotechnology, Santa Cruz, CA) to select the 14-3-3ζ-silenced cell clones. Cells transfected with scrambled shRNA were used as controls.

Microarray processing and analysis

Total RNA from NCI-H1975 cells infected with lentiviruses expressing either scrambled shRNA or 14-3-3ζ-shRNA was extracted using Trizol reagent. The Thermo NanoDrop 2000 and the Agilent 2100 Bioanalyzer were used to assess the quantity and quality of RNA. To define the gene expression profiles, Affymetrix Human GeneChip Primeview (ThermoFisher Science, Catalog number: 902487) was used for microarray analysis according to manufacturer's instructions. An array of raw data

was generated by scanning with a GeneChip Scanner 3000. According to the following criteria, differentially expressed genes between NCI-H1975 cell lines transfected by 14-3-3ζ-shRNA and NCI-H1975 cell lines transfected by scrambled shRNA were selected: $p < 0.001$ and absolute fold change > 4. Pathway enrichment analysis was conducted for differentially expressed genes using Ingenuity Pathway Analysis (IPA, QIAGEN Bioinformatics) commercially available software.

Apoptosis assays

Apoptosis was detected by PE Annexin V/7-Amino-Actinomycin (7-AAD) staining (BD Pharmingen, San Diego, CA, USA) according to the manufacturer's instructions. In brief, cells were washed twice with cold PBS, resuspended in 1X binding buffer at a concentration of 1 x 10^6 cells/ml. 100 µl of the solution (1×10^5 cells) were transfered to a 5 ml culture tube and stained with 5 µl PE Annexin V and 5µl 7-AAD at room temperature for 15 min in the dark. Then 400 µl of 1X Binding Buffer was added to each tube. The apoptotic levels in each sample were analyzed using a LSR II flow cytometer (BD) and FlowJo software (FlowJo, LLC, Bethesda, USA) within 1 hour.

Cell viability assay

The viability of cells was measured using the Cell Counting Kit-8 (CCK-8) (Dojindo Molecular Technologies, Kumamoto, Japan). At a density of 7 × 103 cells per well, the cells were cultured in a 96-well plate and incubated overnight before treatment. After 48 h of growth with different concentrations of gefitinib (0-40 µM), the cells were incubated in 10% CCK-8 solution for an additional 1 h at 37 °C in dark. The absorbance at 450 nm (A450) was examined on a microplate reader (BioTek, Winooski, VT, USA). Three parallel experiments were performed in 5 replicate wells per sample. The IC50 values were determined using IBM SPSS Statistics 20.0 software.

Xenograft models

Animal experiments were performed in accordance with the Institutional Ethics Committee for the Administration of Laboratory Animals of Harbin Medical University, China. 5 × 10^6 H1975/ scr-shRNA cells (vector control) or

H1975/14-3-3ζ-shRNA cells that had been resuspended in 100 μL PBS were injected subcutaneously into the right flanks of the male BALB/c nude mice (Changzhou Cavens Laboratory Animal Co., Ltd.) in each group (n = 10 per group). Tumour volume (V) was calculated with the formula π/6 × larger diameter × (smaller diameter)^2.When established tumors of approximately 75mm3 in diameter were detected, the mice bearing H1975 cells with or without stable knockdown of 14-3-3ζ were randomized into two sub-groups (n = 4 per subgroup) . The mice in each sub-group receive Gefitinib (50 mg/kg) or sterile water by oral gavage every day. Subsequently, xenografted tumor size was monitored every 3 days for 28 days. Tumor weight was measured after excision on the final day of the experiment.

Statistical analysis

All data statistical analyses were performed with SPSS 20.0 software package (SPSS, Chicago, IL, USA) and Graphpad Prism. The results were expressed as the mean± SD (standard deviation) for at least three independent experiments if data were quantitative nature. Continuous variables between two groups were analysed by Student's t-tests. The differences in categorical variables were analysed with χ2 tests. Statistical significance was determined for 2-tailed tests at p <0.05, and described using asterisks (*).

Results

14-3-3ζ expression predicts LUAD and pan-cancer prognosis

We firstly investigate examined 14-3-3ζ expression at the mRNA level in different carcinomas based on the TCGA and GTEx databases [27]. We found that 14-3-3ζ is significantly elevated in 12 kinds of cancer tissuues including LUAD, LUSC, breast invasive carcinoma, cervical squamous cell carcinoma, cholangio carcinoma, colon adenocarcinoma, liver hepatocellular carcinoma, ovarian serous cystadenocarcinoma, pancreatic adenocarcinoma, rectum adenocarcinoma, stomach adenocarcinoma, thymoma tissues, compared to those in non-tumor tissues (Fig. 1a). We further verified 14-3-3ζ expression in LUAD tissues with EGFR-activating mutations using IHC. Consistently, 14-3-3ζ was higher expressed in LUAD tissues than normal

adjacent tissues (Fig. 1b). By Western blot analysis, we also discoveried that 14-3-3ζ expression levels in the LUAD tissues were higher than those observed in the paired non-tumoral lung tissues, respectively (Fig. 1c).

TCGA database was used to detect the prognostic significance of 14-3-3ζ expression in pan-cancer and LUAD. From 9980 tumors across 26 kind of cancers, we showed that high 14-3-3ζ expression was a prognostic factor for overall survival (OS) and disease-free survival (DFS) in pan-cancer (Fig. 1d). Moreover, we found that high 14-3-3ζ expression was associated with poor survival for LUAD patients (Fig. 1e). Using Kaplan–Meier plotter online tool [28], the curves consistently depicted that patients with increased levels of 14-3-3ζ expression had shorter OS and post progression survival (PPS) than those with low 14-3-3ζ expression levels (Supplementary Fig.1).

The clinicopathological signature of 14-3-3ζ in LUAD with EGFR-activating mutations.

Next, we intevestgated the clinicopathological signature of 14-3-3ζ and the relathionship between 14-3-3ζ expression and EGFR-TKI responsiveness in LUAD with EGFR-activating mutations. The protein expression level of 14-3-3ζ was classified as low or high based on the intensity and proportion of positively stained cells in these specimens (Fig. 2a). Our IHC analysis results dislosed that high 14-3-3ζ expression was significantly associated with advanced T stage, TNM stage, present of lymph node metastasis (Fig. 2b-d; Supplementary Table S1). Of note, 14-3-3ζ was higher expressed in the EGFR-TKI-refractory specimens (PFS $<$ 6 months) than that in the EGFR-TKI-sensitive group (PFS $\geqslant$ 6 months) by IHC (Fig. 2e; Supplementary Table S1). Our results indicated that 14-3-3ζ exprssion could play a role in EGFR-TKI resistance.

Knockdown of 14-3-3ζ sensitizes gefitinib-resistant LUAD cells to gefitinib

To identify whether 14-3-3ζ is relevant to EGFR-TKI resistance, Western blot analyses were performed to measure the 14-3-3ζ protein levels in EGFR-TKI sensitive LUAD cell line (PC-9) and its EGFR-TKI-resistant daughter cell line (PC-9/GR). Higher expression of 14-3-3ζ protein was found in PC-9/GR than that in

PC-9 (Fig. 3a). Next, in PC-9/GR and H1975 cells harboring an EGFR L858R/T790M mutation, expression vectors containing short hairpin RNAs (shRNAs) targeting 14-3-3ζ was used to decrease 14-3-3ζ expression. As shown in Figure 3b, 14-3-3ζ shRNA-transfected EGFR-TKI-resistant cells (14-3-3ζ-shRNA) displayed a significant decrease in expression of 14-3-3ζ compared to control group (Ctrl).

Knockdown of 14-3-3ζ sensitized PC-9/GR and H1975 cells to different concentrations of gefitinib (Fig. 3c). Similar finding was observed in flow cytometric analysis, wherein 14-3-3ζ-shRNA cancer cells exhibited a higher rate of apoptosis and were sensitive to gefitinib treatment (Fig. 3d). To further investegated whether 14-3-3ζ-shRNA in combination with gefitinib has a better inhibitory effect on tumor cell motility, invasion and migration than gefitinib alone, we performed transwell assay and wound healing. Transwell assays revealed that knocking down 14-3-3ζ inhibited LUAD cell migration and invasion compared with control cells when combined with gefitinib (Fig. 3e). Consistent with the results of Transwell assays, the cells transfected with 14-3-3ζ specifc shRNA were slower to close scratch wounds than control when all cells were treated with gefitinib (Fig. 3f). In summary, these *in vitro* data suggest that the combined 14-3-3ζ knockdown and gefitinib sensitizes resistant cells to EGFR-TKI and overcomes the resistance in EGFR-TKI-resistant cells.

14-3-3ζ knockdown inhibits EMT and BMP2/Smad/ID-1 signaling activation

Next, we sought to explore the potential mechanism by which 14-3-3ζ knockdown regulates EGFR-TKI resistance. EMT was involved in the phenotypic changes which were identified as one of EGFR-TKI resistance mechanisms [29, 30]. 14-3-3ζ deleption in EGFR-TKI-resistant cells led to upregulation of epithelial markers (E-cadherin) and downregulation of mesenchymal markers (N-cadherin) and Vimentin (Fig. 4a).

Furthermore, we determined global gene expression profiling of in EGFR-TKI-resistant cells, H1975, infected with lentivirus expressing either Scr-shRNA or 14-3-3ζ-shRNA using microarray analysis. We identified 601 differentially expressed genes ($p < 0.001$ and absolute fold change > 1.5), which

included 363 up-regulated genes and 238 downregulated genes after 14-3-3ζ knockdown (Fig. 4b).Using commercially available IPA software, we found that 14-3-3ζ knockdown affected a wide range of cellular functions (Supplementary Table S2) and canonical pathways (Supplementary Table S3). The absolute value of Z score of canonical pathways which the greater than 2 was ranked (Fig. 4c). BMP signaling pathway notely was downregulated by 14-3-3ζ-shRNA, suggesting 14-3-3ζ could positively regulate BMP signaling pathway. In detail, BMP2/BMPR2/p-Smad (1/5)/ID1 axis was mediated by 14-3-3ζ knockdown by microarray technology (Fig. 4d). The same finding was observed in EGFR-TKI-resistant cells using Western blot (Fig. 4e). In addition, a positive correlation between 14-3-3ζ and BMPR2, Smad5 was observed in the LUAD samples from the TCGA database (Fig. 4f).

To investigate the correlation between 14-3-3ζ expression and ID1 in LUAD patients with EGFR-mutant, the expression of ID1 was detected. The protein expression level of ID1 in these cases was also classified as low or high based on the intensity and proportion of positively stained cells in the IHC analysis (Supplementary Fig. S2; Fig. 4g, left). In line with our findings in the tumor cell lines, the distribution and intensity of 14-3-3ζ were positively correlated with ID1 in specimens of human EGFR-mutant LUAD (Fig. 4g, right).

14-3-3ζ silencing sensitizes EGFR mutant LUAD cells to gefitinib *in vivo*.

To determine the role of 14-3-3ζ on the sensitivity of EGFR mutant LUAD cells to gefitinib *in vivo*, we injected into the ventral region of non-obese diabetic (NOD)-severe combined immunodeficient (SCID) mice with 14-3-3ζ-shRNA or Ctrl when treated with gefitinib or PBS. Gefitinib treatment alone had little effect on inhibitory of tumor growth. Interestingly, 14-3-3ζ-shRNA alone was able to suppress tumor growth, and could further enhance the effect when combined with gefitinib (Fig. 5; Supplementary Fig. S3). These results indicate that knockdown of 14-3-3ζ sensitizes LUAD cells to gefitinib therapy *in vivo*.

Discussion

EGFR-TKI therapies have shown diverse clinical benefit and the overall responses range from 5 to 90% [31]. Thus, the work to elucidate the cancer heterogeneity which

impacted remission to EGFR-TKI could be crucial to develop new therapeutic strategies with better efficacy for LUAD patients with EGFR-activating mutations [32].

In the present study, we firstly demenstrated that 14-3-3ζ expression was elevated and predicted unfavourable prognosis in pan-cancer based on TCGA. We found that high 14-3-3ζ expression was significantly associated with advanced T stage, TNM stage, the present of lymph node metastasis and poor treatment response to EGFR-TKI in LUAD patients with EGFR-activating mutations. Our study provide a molecular rationale for an unappreciated role of 14-3-3ζ in promoting EGFR-TKI resistance accompanied by EMT. Additionally, we showed that 14-3-3ζ positively regulated BMP2/Smad/ID-1 signaling.

14-3-3ζ as a central hub in signaling networks exerts its functions by the serine/threonine phosphorylation event involved in multiple cellular processes [8, 11, 33]. Overexpression of 14-3-3ζ been reported to contribute to tumor progression of various malignancies by regulating migration, cell-cycle progression, apoptosis, differentiation, metabolism and so on of cancer cells [11-14, 16, 34]. Consistently, we found that the expression of 14-3-3ζ which was related to the product of oncogene was elevated in pan-cancer and correlated with worse clinical stage and surival of LUAD. Multiple lines of evidence reveal the oncogenic actor of 14-3-3ζ as promising predictor of progression and a prognostic biomarker in patients with lung cancer [35-39]. The previous studies and our work emphasized the promising role of 14-3-3ζ as a novel target in the therapies of lung cancer even pan-cancer [8].

Here, we firstly denmonstrated that suppression of 14-3-3ζ in LUAD cells enhanced sensitivity to EGFR-TKI. The molecular mechanisms which have been found to confer resistance to first- and second-generation EGFR-TKI included the acquisition of EGFR T790M mutation, MET amplification, HER-2 amplification, AXL activation, aberrant PI3K/AKT pathway, phenotypic transformation such as EMT [40-42]. 14-3-3ζ was disclosed to regulate the PI3K/Akt pathway by enhancing Akt phosphorylation via binding to the p85α regulatory subunit of PI3K [43, 44]. Whether

14-3-3ζ promotes EGFR-TKI resistance through PI3K/Akt pathway was further investigated in a future study.

Lung cancer cells with acquired resistance to gefitinib or osimertinib (AZD9291) showed EMT characteristics, with a decrease in E-cadherin, and increases in mesenchymal markers and stemness without any EGFR secondary mutations [45]. Considering the impact of EMT on EGFR-TKI resistance, we confirmed 14-3-3ζ-induced EMT in this study. In agreement with our results, increased expression of 14-3-3ζ promoted EMT phenotype of cancer cells [13-15]. 14-3-3ζ stabilized TGFβ RI, thereby activating the TGFβ/Smad pathway involved in EMT [15]. In breast cancer, 14-3-3ζ cooperates with ErbB2 to promote progression of ductal carcinoma in situ to invasive breast cancer by inducing EMT [14]. In lung cancer, 14-3-3ζ prevented β-catenin ubiquitination and degradation, and subsequently inducing EMT progress and invasiveness [13]. Our results could help to improve therapeutic intervention and 14-3-3ζ/EMT could serve as biomarkers in guiding the selection of patients who may particularly benefit from EGFR-TKI.

As far as we know, we firstly illuminated that the role of 14-3-3ζ in regulation of BMP2/Smad/ID-1 signaling. Based on structural and functional affnities, more than ten BMPs have been defined in the relative ones of TGFβ family [18]. The BMP and TGFβ pathways intersect at various signaling hubs and cooperatively or counteractively participate in multiple cellular processes in cancer [18, 46]. Interestingly, our microarray analysis results and previous studies showed that TGFβ pathways was regulated by 14-3-3ζ [14, 15, 36]. It was reasonable to discover the impact of 14-3-3ζ on BMP2/Smad/ID-1 signaling. The detailly regulatory mechanisms need to be further elucidated. Because the sustained expression of ID1 induced EMT in previous studies, we think that 14-3-3ζ promotes gefitinib resistance and EMT by BMP2/Smad/ID-1 signaling [24, 46].

Conclusion

Take together, we uncovered an unappreciated role of 14-3-3ζ in EGFR-TKI resistance *in vitro* and *in vivo*. In addition, 14-3-3ζ potentiated EMT and

BMP2/Smad/ID-1 signaling. This work could help to predict and guide therapeutic responsiveness of EGFR-TKI in LUAD. Our findings suggest that targeting 14-3-3ζ/BMP pathway/EMT could be a potential therapeutic strategy to reverse the EGFR-TKIs resistance in LUAD patients with acquired resistance.

Abbreviations

LUAD: lung adenocarcinoma;

IHC: immunohistochemistry;

EGFR-TKI: epidermal growth factor receptor-tyrosine kinase inhibitor;

EMT: epithelial-to-mesenchymal transition

BMPs: Bone morphogenetic proteins;

ID1: inhibitors of differentiation 1;

Declarations

Ethics approval and consent to participate

LUAD tissues were collected from patients who underwent surgical resection at the Harbin Medical University Cancer Hospital (Harbin, China). All patients signed consent letters and all manipulation of the tissues was approved by the Ethics Committee of Harbin Medical University. All experiments were performed in accordance with the guidelines of the Harbin Medical University.

All animal experiments were carried out in accordance with the National Institutes of Health guide for the care and use of Laboratory animals (NIH Publications No. 8023, revised 1978) and the guidelines of the Harbin Medical University.

Consent for publication

We have obtained consents to publish this paper from all the participants of this study.

Availability of data and materials

All data generated or analysed during this study are included in this published article [and its supplementary information files].

Competing interests

The authors declare that they have no competing interests.

Acknowledgements

Not applicable.

Funding

This work was supported in part by National Natural Science of China grants (No.81602717 to HL and No.81972162 to JH), Natural Science and Technology Foundation of Heilongjiang Province (No.LC201439 to HL and No.H201406 to YC), Postdoctoral Foundation of Heilongjiang Province (No.LBH-Z15182 to HL) and the 7th Postdoctoral Special Science-research Fund of Heilongjiang Province (No.LBH-TZ1616 to JH).

Authors' contributions

JC, YS and XH performed experiments, analyzed data, and wrote the paper. They contributed equally to this work. HL and LC designed this research. JH and XC helped with the IHC assay. YC and XX helped with cell culture, western blot experiments. HL and YX critically revised the manuscript. All authors read and approved the final manuscript.

References

1. Siegel R L, Miller K D. Cancer statistics, 2019. 2019;69:7-34.
2. Bray F, Ferlay J, Soerjomataram I, et al. Global cancer statistics 2018: GLOBOCAN estimates of incidence and mortality worldwide for 36 cancers in 185 countries. CA Cancer J Clin 2018;68:394-424.
3. Sivakumar S, Lucas F A S, McDowell T L, et al. Genomic Landscape of Atypical Adenomatous Hyperplasia Reveals Divergent Modes to Lung Adenocarcinoma. Cancer Res 2017;77:6119-6130.
4. Herbst R S, Heymach J V, Lippman S M. Lung cancer. N Engl J Med 2008;359:1367-80.
5. Heist R S, Engelman J A. SnapShot: non-small cell lung cancer. Cancer Cell 2012;21:448.e2.
6. Greulich H. The genomics of lung adenocarcinoma: opportunities for targeted therapies. Genes Cancer 2010;1:1200-10.

7. Pennington K L, Chan T Y, Torres M P, et al. The dynamic and stress-adaptive signaling hub of 14-3-3: emerging mechanisms of regulation and context-dependent protein-protein interactions. Oncogene 2018;37:5587-5604.
8. Matta A, Siu K W, Ralhan R. 14-3-3 zeta as novel molecular target for cancer therapy. Expert Opin Ther Targets 2012;16:515-23.
9. Lim G E, Albrecht T, Piske M, et al. 14-3-3zeta coordinates adipogenesis of visceral fat. 2015;6:7671.
10. Lim G E, Piske M, Lulo J E, et al. Ywhaz/14-3-3zeta Deletion Improves Glucose Tolerance Through a GLP-1-Dependent Mechanism. Endocrinology 2016;157:2649-59.
11. Neal C L, Yu D. 14-3-3zeta as a prognostic marker and therapeutic target for cancer. Expert Opin Ther Targets 2010;14:1343-54.
12. Niemantsverdriet M, Wagner K, Visser M, et al. Cellular functions of 14-3-3 zeta in apoptosis and cell adhesion emphasize its oncogenic character. Oncogene 2008;27:1315-9.
13. Chen C H, Chuang S M, Yang M F, et al. A novel function of YWHAZ/beta-catenin axis in promoting epithelial-mesenchymal transition and lung cancer metastasis. Mol Cancer Res 2012;10:1319-31.
14. Lu J, Guo H, Treekitkarnmongkol W, et al. 14-3-3zeta Cooperates with ErbB2 to promote ductal carcinoma in situ progression to invasive breast cancer by inducing epithelial-mesenchymal transition. Cancer Cell 2009;16:195-207.
15. Hong H Y, Jeon W K, Bae E J, et al. 14-3-3 sigma and 14-3-3 zeta plays an opposite role in cell growth inhibition mediated by transforming growth factor-beta 1. Mol Cells 2010;29:305-9.
16. Murata T, Takayama K, Urano T, et al. 14-3-3zeta, a novel androgen-responsive gene, is upregulated in prostate cancer and promotes prostate cancer cell proliferation and survival. Clin Cancer Res 2012;18:5617-27.
17. Neal C L, Yao J, Yang W, et al. 14-3-3zeta overexpression defines high risk for breast cancer recurrence and promotes cancer cell survival. Cancer Res 2009;69:3425-32.
18. Dituri F, Cossu C, Mancarella S. The Interactivity between TGFbeta and BMP Signaling in Organogenesis, Fibrosis, and Cancer. 2019;8
19. Langenfeld E M, Bojnowski J, Perone J, et al. Expression of bone morphogenetic proteins in human lung carcinomas. Ann Thorac Surg 2005;80:1028-32.
20. Chu H, Luo H, Wang H, et al. Silencing BMP-2 expression inhibits A549 and H460 cell proliferation and migration. Diagn Pathol 2014;9:123.
21. Yang M, Fan Z, Wang F, et al. BMP-2 enhances the migration and proliferation of hypoxia-induced VSMCs via actin cytoskeleton, CD44 and matrix metalloproteinase linkage. Exp Cell Res 2018;368:248-257.
22. Gautschi O, Tepper C G, Purnell P R, et al. Regulation of Id1 expression by SRC: implications for targeting of the bone morphogenetic protein pathway in cancer. Cancer Res 2008;68:2250-8.
23. Li J, Li Y, Wang B, et al. Id-1 promotes migration and invasion of non-small cell lung cancer cells through activating NF-kappaB signaling pathway. J Biomed Sci 2017;24:95.

24. Castanon E, Soltermann A, Lopez I, et al. The inhibitor of differentiation-1 (Id1) enables lung cancer liver colonization through activation of an EMT program in tumor cells and establishment of the pre-metastatic niche. Cancer Lett 2017;402:43-51.
25. Bhattacharya R, Kowalski J, Larson A R, et al. Id1 promotes tumor cell migration in nonsmall cell lung cancers. J Oncol 2010;2010:856105.
26. Yuen H F, Chan Y P, Chan K K, et al. Id-1 and Id-2 are markers for metastasis and prognosis in oesophageal squamous cell carcinoma. Br J Cancer 2007;97:1409-15.
27. Wei C Y, Wang L, Zhu M X, et al. TRIM44 activates the AKT/mTOR signal pathway to induce melanoma progression by stabilizing TLR4. J Exp Clin Cancer Res 2019;38:137.
28. Nagy A, Lanczky A, Menyhart O, et al. Validation of miRNA prognostic power in hepatocellular carcinoma using expression data of independent datasets. 2018;8:9227.
29. Soucheray M, Capelletti M, Pulido I, et al. Intratumoral Heterogeneity in EGFR-Mutant NSCLC Results in Divergent Resistance Mechanisms in Response to EGFR Tyrosine Kinase Inhibition. Cancer Res 2015;75:4372-83.
30. Huang J, Lan X, Wang T, et al. Targeting the IL-1beta/EHD1/TUBB3 axis overcomes resistance to EGFR-TKI in NSCLC. Oncogene 2019
31. Yao Z, Fenoglio S, Gao D C, et al. TGF-beta IL-6 axis mediates selective and adaptive mechanisms of resistance to molecular targeted therapy in lung cancer. Proc Natl Acad Sci U S A 2010;107:15535-40.
32. Shimamura T. Heterogeneity in Tumors and Resistance to EGFR TKI Therapy-Response. Cancer Res 2016;76:3111.
33. Jansen S, Melkova K, Trosanova Z, et al. Quantitative mapping of microtubule-associated protein 2c (MAP2c) phosphorylation and regulatory protein 14-3-3zeta-binding sites reveals key differences between MAP2c and its homolog Tau. J Biol Chem 2017;292:10316.
34. Choi J E, Hur W, Jung C K, et al. Silencing of 14-3-3zeta over-expression in hepatocellular carcinoma inhibits tumor growth and enhances chemosensitivity to cis-diammined dichloridoplatium. Cancer Lett 2011;303:99-107.
35. Xue M, Tao W. Upregulation of MUC1 by its novel activator 14-3-3zeta promotes tumor invasion and indicates poor prognosis in lung adenocarcinoma. Oncol Rep 2017;38:2637-2646.
36. Zhao Y, Qiao W, Wang X, et al. 14-3-3zeta/TGFbetaR1 promotes tumor metastasis in lung squamous cell carcinoma. Oncotarget 2016;7:82972-82984.
37. Tong S, Xia T, Fan K, et al. 14-3-3zeta promotes lung cancer cell invasion by increasing the Snail protein expression through atypical protein kinase C (aPKC)/NF-kappaB signaling. Exp Cell Res 2016;348:1-9.
38. Zang D, Li X, Zhang L. 14-3-3zeta Overexpression and abnormal beta-catenin expression are associated with poor differentiation and progression in stage I non-small cell lung cancer. Clin Exp Med 2010;10:221-8.
39. Fan T, Li R, Todd N W, et al. Up-regulation of 14-3-3zeta in lung cancer and its implication as prognostic and therapeutic target. Cancer Res 2007;67:7901-6.
40. Lim S M, Syn N L, Cho B C, et al. Acquired resistance to EGFR targeted therapy in

non-small cell lung cancer: Mechanisms and therapeutic strategies. Cancer Treat Rev 2018;65:1-10.

41. Zhu X, Chen L, Liu L, et al. EMT-Mediated Acquired EGFR-TKI Resistance in NSCLC: Mechanisms and Strategies. Front Oncol 2019;9:1044.

42. Sos M L, Koker M, Weir B A, et al. PTEN loss contributes to erlotinib resistance in EGFR-mutant lung cancer by activation of Akt and EGFR. Cancer Res 2009;69:3256-61.

43. Castaneda A, Serrano C, Hernandez-Trejo J A, et al. pVHL suppresses Akt/beta-catenin-mediated cell proliferation by inhibiting 14-3-3zeta expression. Biochem J 2017;474:2679-2689.

44. Neal C L, Xu J, Li P, et al. Overexpression of 14-3-3zeta in cancer cells activates PI3K via binding the p85 regulatory subunit. Oncogene 2012;31:897-906.

45. Weng C H, Chen L Y, Lin Y C, et al. Epithelial-mesenchymal transition (EMT) beyond EGFR mutations per se is a common mechanism for acquired resistance to EGFR TKI. Oncogene 2019;38:455-468.

46. Huang Y H, Hu J, Chen F, et al. ID1 mediates escape from TGF-beta tumor suppression in pancreatic cancer. 2019

Figures

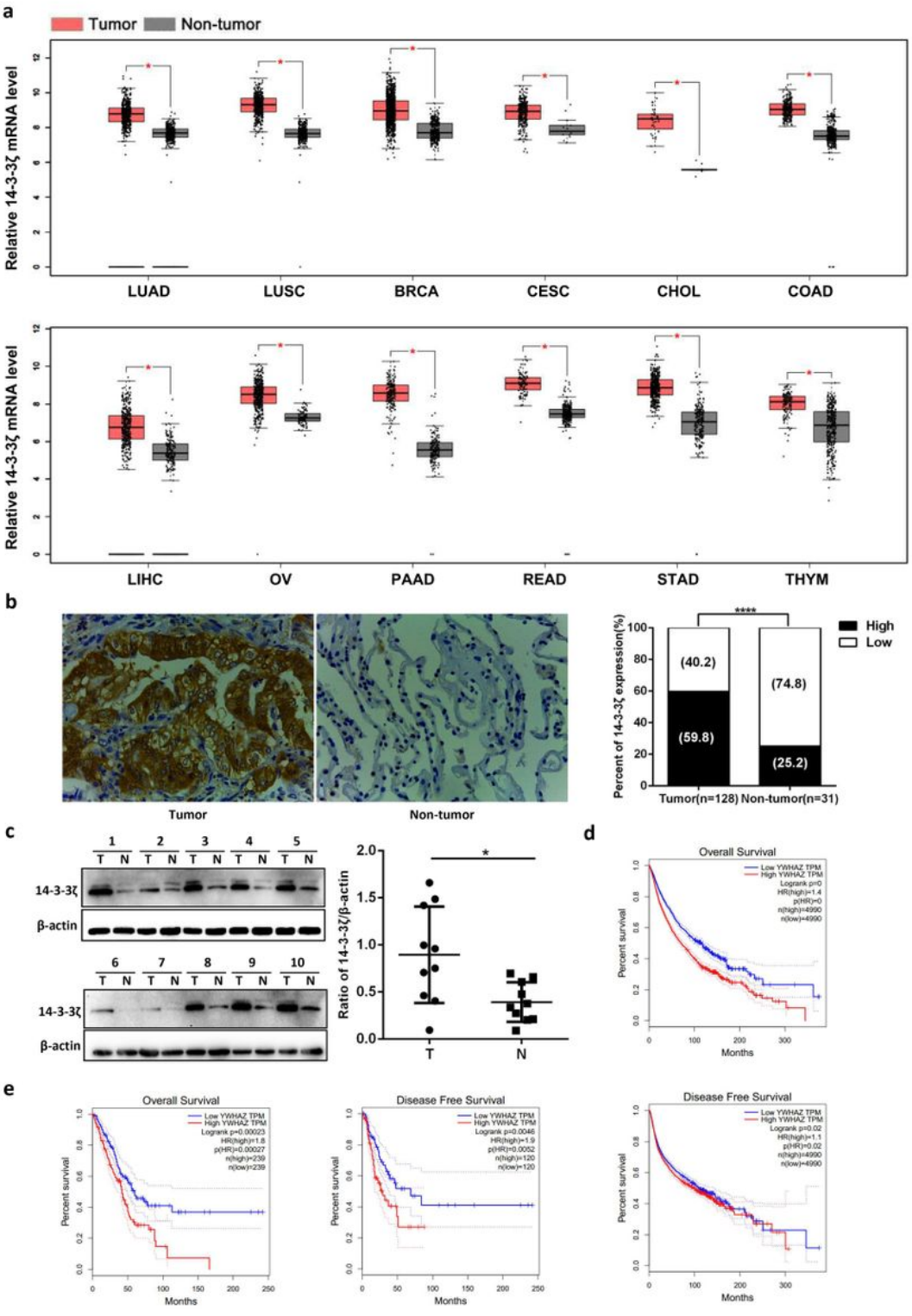

Figure 2

Elevated 14-3-3ζ expression positively correlates with poor prognosis of LUAD patients. (a) Relative mRNA levels of 14-3-3ζ in different tumors were analyzed by GEPIA. (b) Representative immunostaining images for 14-3-3ζ expression in 128 human LUAD tissues with EGFR mutant (Tumor) and 31 normal

LUAD tissues (Nontumor). Original magnification, ×400.Histogram showing percentages of 14-3-3ζ expression for tumor and non-tumor tissues. (c) Western blot analysis of 14-3-3ζ expression in lysates originating from 10 human LUAD samples with EGFR mutant (T) and matched adjacent tissues (N). Right panel: quantification of relative expression levels of 14-3-3ζ. β-actin was used as a loading control. (d) Kaplan-Meier analysis of overall and disease-free survival for high and low 14-3-3ζ expression levels in pan-cancer determined from the GEPIA. (e) Kaplan-Meier analysis of overall and disease-free survival for high and low 14-3-3ζ expression levels in LUAD determined from the GEPIA. (*p<0.05, **p<0.01, ***p<0.001, ****p<0.0001)

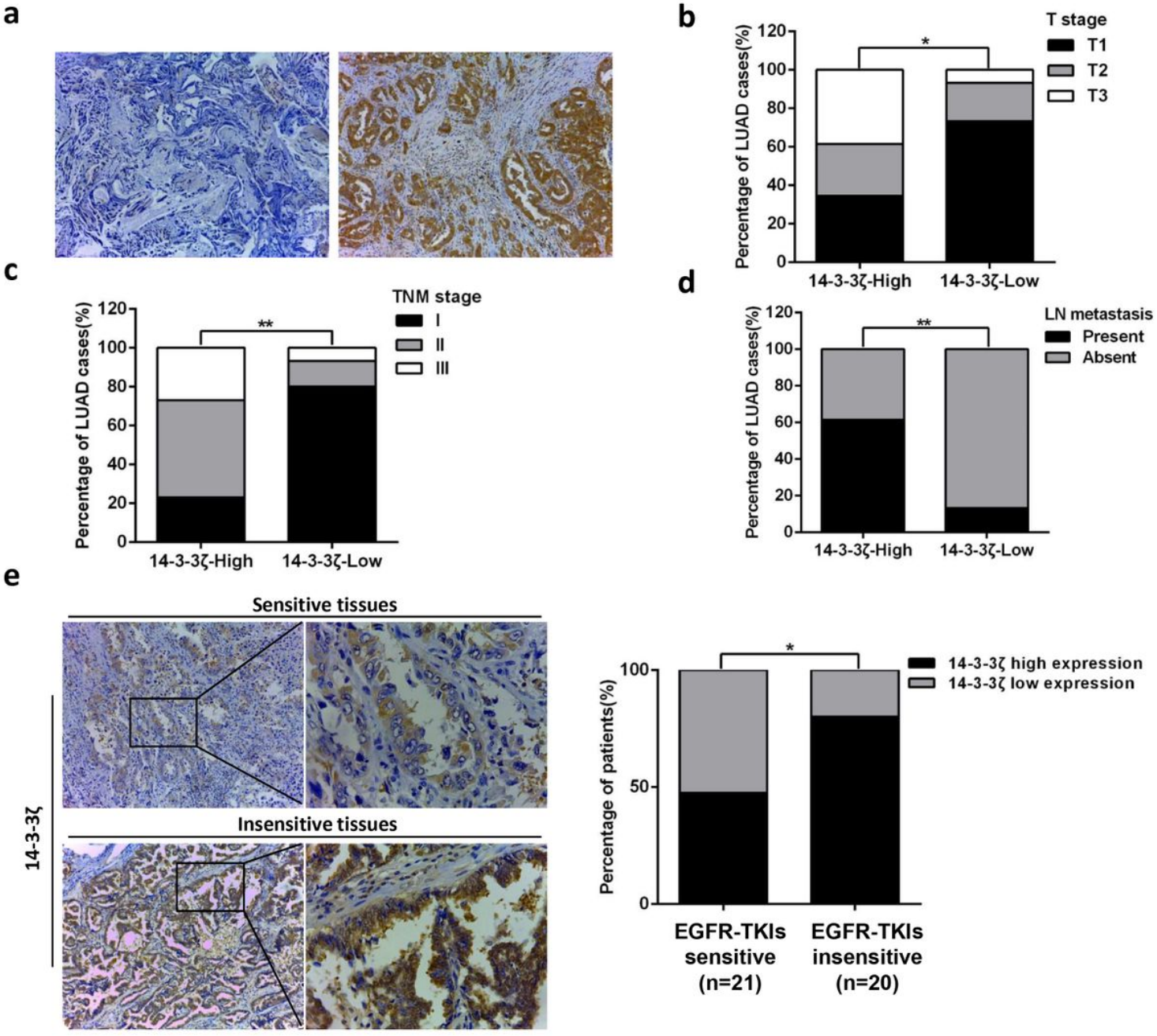

Figure 4

The clinicopathological signature of 14-3-3ζ in LUAD with EGFR-activating mutations. (a) Representative immunohistochemistry staining images of low expression and high expression of 14-3-3ζ in LUAD tissues. Magnification, ×100. (b)The protein expression level of 14-3-3ζ was classified as low or high based on the intensity and proportion of positively stained cells in these specimens. The percentages of patients with different T stage were assigned according to the expression level of 14-3-3ζ. (c) The percentages of patients with different TNM stage were assigned according to the expression level of 14-3-3ζ. (d)The percentages of patients with and without lymph node metastasis were assigned according to the expression level of 14-3-3ζ. (e) Representative immunostaining profiles of 14-3-3ζ in drug-sensitive (PFS≥6 months, n = 21) and drug-insensitive (PFS<6 months, n = 20) LUAD tissues. Magnification, ×100 and ×400(left panel). The percentages of patients with high expression (black bar) and low expression of 14-3-3ζ (grey bar) were assigned according to different responses to EGFR-TKI (right panel). (*p<0.05, **p<0.01, ***p<0.001, ****p<0.0001)

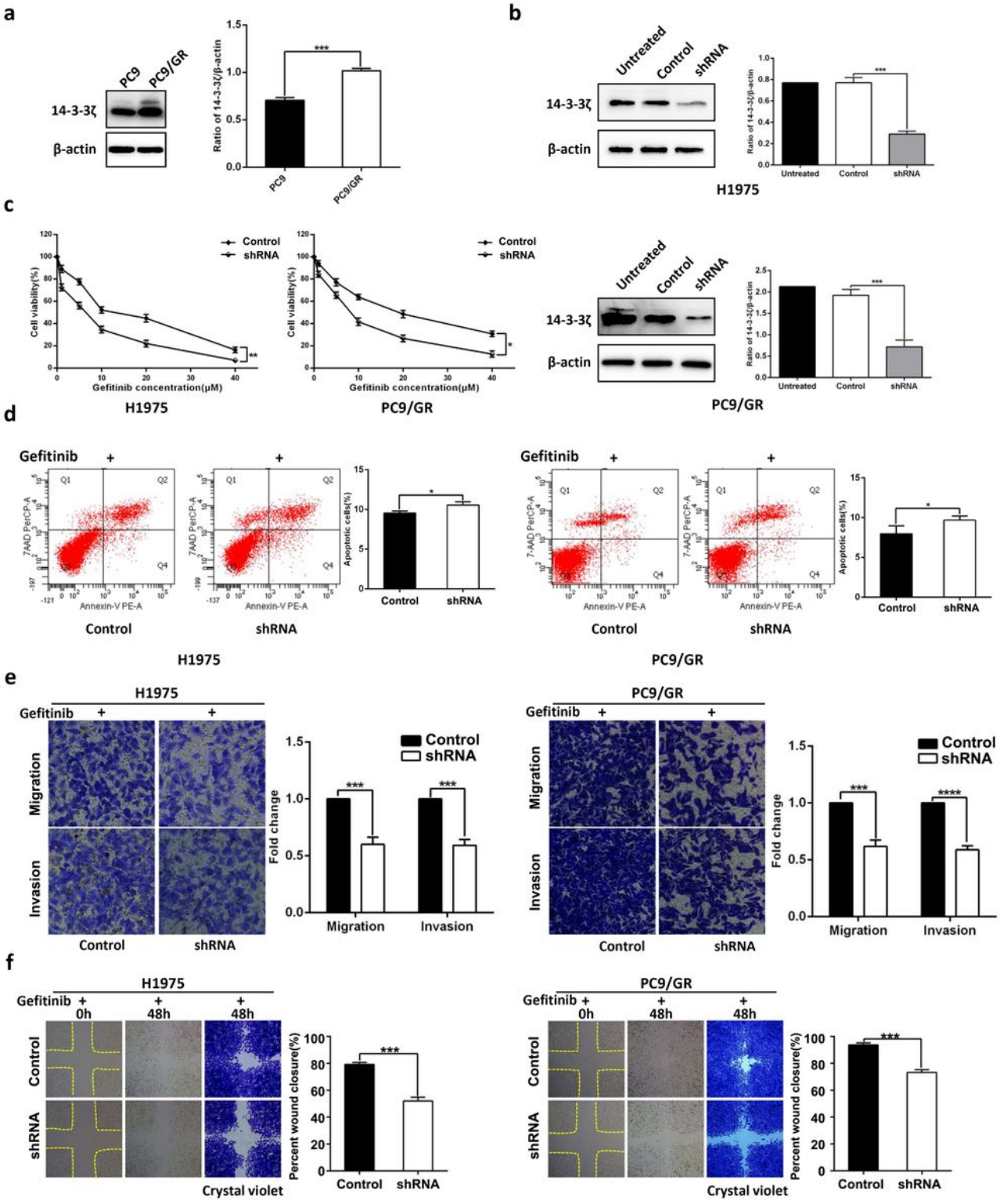

Figure 6

14-3-3ζ knockdown overcomes EGFR-TKI resistance in EGFR-mutant LUAD cells. (a) 14-3-3ζ protein expression levels in PC9 and PC9/GR cell lines as determined by western blot analysis. Histogram showing quantification of relative expression levels of 14-3-3ζ. β-actin was used as a loading control. (b)Western blot analyses of 14-3-3ζ protein expression levels in NCI-H1975 and PC9/GR cells and in cells transfected with Scrambled shRNA (Control) or 14-3-3ζ-shRNA (shRNA). (c) H1975/14-3-3ζ-shRNA (left

panel), PC9/GR/14-3-3ζ-shRNA (right panel) and corresponding vector control cells were treated with the indicated doses of gefitinib for 48 h, and cell viability was analyzed by a CCK-8 assay. (d) Flow cytometric analysis of apoptosis in the indicated cells treated with gefitinib as assessed by Annexin V and 7-AAD staining. A representative flow profile is shown (left panel), and a summary of the percentage of Annexin V-positive cells is shown (right panel). (e) Transwell assays were conducted to assess TKI-resistant cell migration and invasion after 14-3-3ζ knockdown in cells cultured in the presence of gefitinib compared with those of corresponding vector control cells (i.e., crystal violet staining of migratory and invasive cells). Original magnification, ×100. (f) A wound healing assay was performed in the indicated cells as described in e. Original magnification, ×100. (*p<0.05, **p<0.01, ***p<0.001, ****p<0.0001)

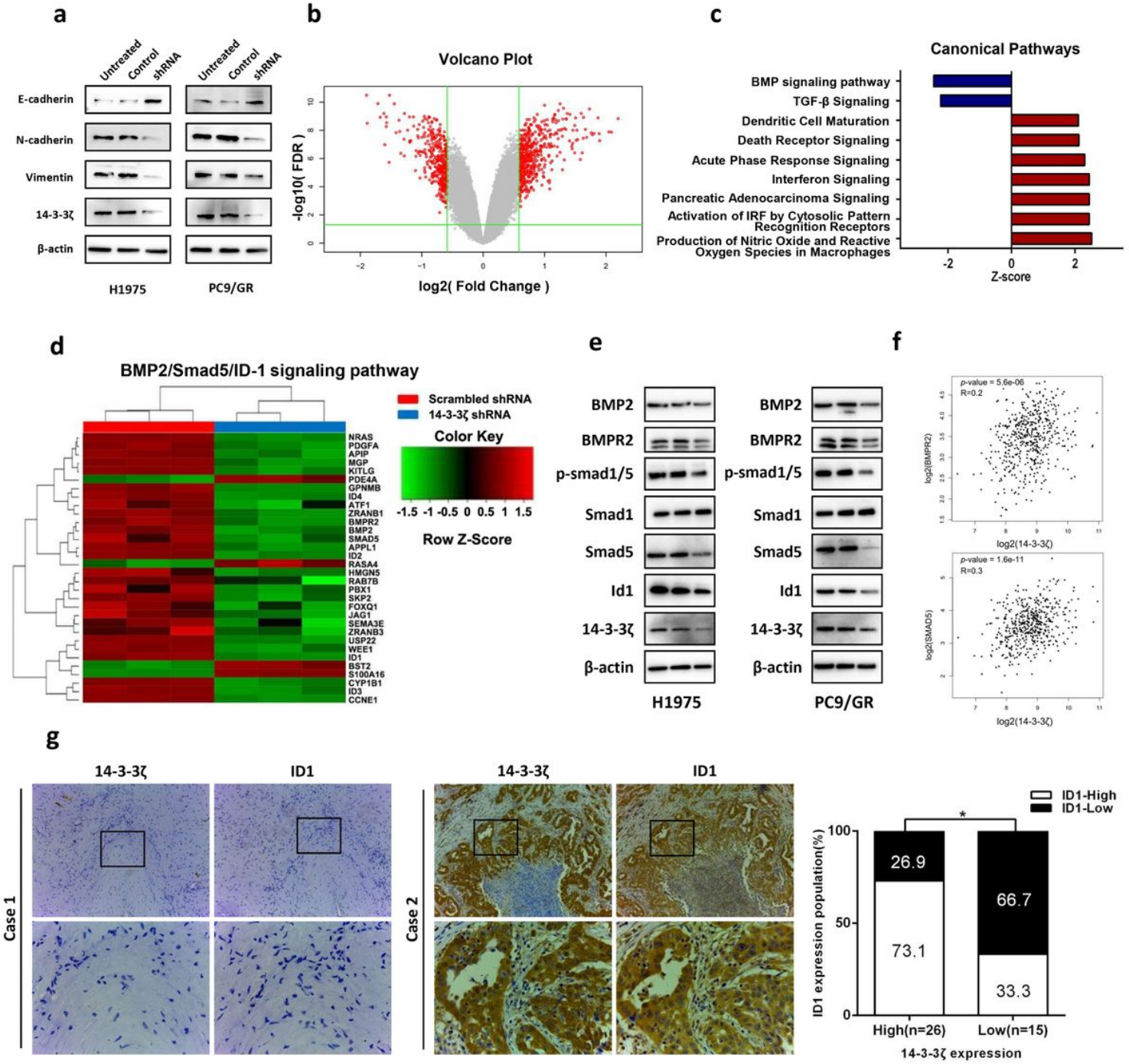

Figure 8

14-3-3ζ knockdown inhibits EMT and BMP pathway in TKI-resistant cells. (a) Western blot analysis of E-cadherin, N-cadherin and Vimentin expression in TKI-resistant cells and 14-3-3ζ-knockdown cells. β-actin was used as a loading control. (b) NCI-H1975 cells infected with lentivirus expressing either scrambled-shRNA or 14-3-3ζ-shRNA. Volcano plots are used to show genes with significant differences in data from two sets of samples in a gene chip. The abscissa is the multiple of the difference (logarithmic transformation with a base of 2), the ordinate is the significant FDR (logarithmic transformation with a base of 10), and the red dots represent genes with significant differences. It was selected based on the absolute value of Fold Change ≥1.5 and FDR <0.05. The gray dots represent other genes that have no significant difference. (c) The bar graph shows the significant enrichment of differentially expressed genes in the classical signaling pathways. According to IPA's internal algorithms and standards, Z-score ≥ 2 means that the pathway is significantly activated, and Z-score ≤-2 means that the pathway is significantly inhibited. (d) Heatmap showing the differential expression of BMP2/Smad5/ID-1 pathway gene signatures in NCI-H1975 cells infected with lentivirus expressing either scrambled-shRNA (blue) or 14-3-3ζ-shRNA (red). Genes and samples are listed in the rows and columns, respectively. A color key for the normalized expression data is shown at the top of the microarray heatmap (green represents downregulated genes; red represents upregulated genes). (e) NCI-H1975 and PC9/GR cells were transfected with 14-3-3ζ-shRNA (shRNA), scrambled shRNA(control), or left untreated (Untreated). Expression levels of BMP2, BMPR2, p-smad1/5, Smad1, Smad5 and Id1 were determined using Western blot. (f)The correlation between 14-3-3ζ and BMPR2, Smad5 mRNA expression was identified by the TCGA database. (g) Representative images of immunohistochemical staining for 14-3-3ζ and ID1 in serial sections of LUAD samples from patients. Case 1 is representative of a patient with non-14-3-3ζ-overexpressing lung cancer, whereas Case 2 is representative of a patient with 14-3-3ζ-overexpressing LUAD (left panel). A statistically significant correlation between 14-3-3ζ-high expression and ID1-high expression in 41 cases of LUAD tissues. The expression levels of 14-3-3ζ and ID1 were determined by immunostaining (right panel). Magnification, ×100 and ×400. (*p<0.05)

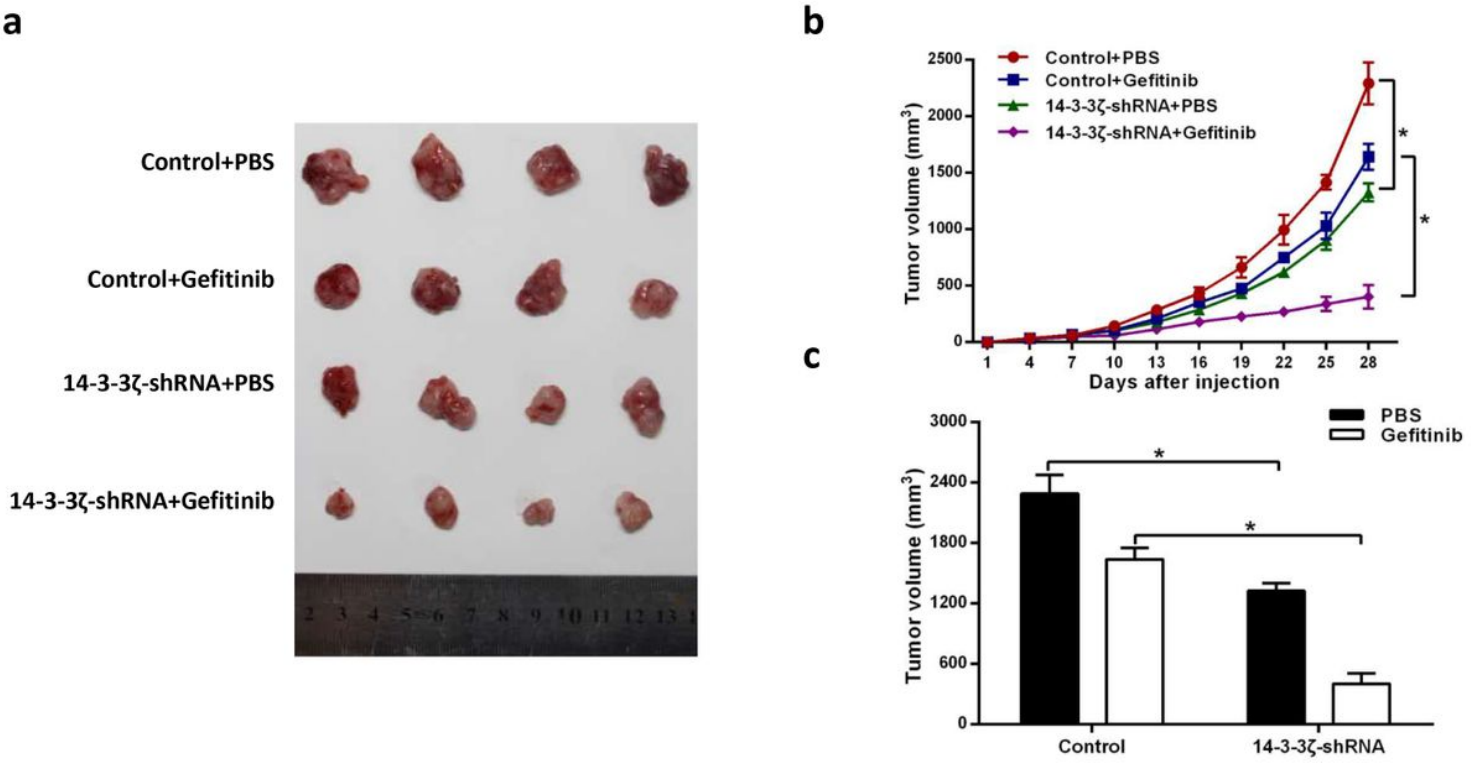

Figure 10

14-3-3ζ silencing enhances the sensitivity of EGFR mutant LUAD to EGFR-TKIs in a mouse xenograft model. (a) Representative images of tumors at 28 days after inoculation using H1975/Control or H1975/14-3-3ζ-shRNA cells treated with PBS or gefitinib. Control group, mice inoculated with H1975/scrambled-shRNA cells; 14-3-3ζ-shRNA group, mice inoculated with 14-3-3ζ silenced H1975 cells; Control + gefitinib group, mice inoculated with control H1975 cells and treated with gefitinib; 14-3-3ζ-shRNA + gefitinib, mice inoculated with 14-3-3ζ silenced H1975 cells and treated with gefitinib. (b) Tumor growth curves in the nude mice injected with H1975/Control or H1975/14-3-3ζ-shRNA cells treated with PBS or gefitinib. N = 4 for each group. (c) Tumor volumes at day 28 after the inoculation. Left (black column), average tumor volumes at day 28 after inoculation with H1975/Control or H1975/14-3-3ζ-shRNA cells in mice treated with PBS; right (white column), average tumour volumes at day 28 after inoculation of H1975/Control or H1975/14-3-3ζ-shRNA cells in mice treated with gefitinib. (*p<0.05)

Supplementary Files

This is a list of supplementary files associated with this preprint. Click to download.

- SupplementaryFigureS2.jpg
- SupplementaryFigureS2.jpg
- SupplementaryFigureS3.jpg
- SupplementaryFigureS1.jpg

- SupplementaryTableS2.xls
- SupplementaryTableS3.xlsx
- SupplementaryTableS1.docx
- SupplementaryFigureS3.jpg
- SupplementaryTableS2.xls
- SupplementaryTableS3.xlsx
- SupplementaryFigureS1.jpg
- SupplementaryTableS1.docx